Supporting information

1 Characterization

All reagents and chemicals were commercially available and used without further purification unless otherwise stated. UV-vis absorption spectra of the polymer solution and films were recorded on a Shimadzu UV-2600 UV-VIS spectrophotometer. Cyclic voltammetry of films was performed on a computer-controlled CHI 660E electrochemical workstation at a scanning rate of 50 mV/s under argon atmosphere using Ar-saturated solution of 0.1 mol/L tetra(*n*-butyl) ammonium hexafluorophosphate (Bu_4NPF_6) in acetonitrile (CH_3CN) as the supporting electrolyte. A glassy carbon working electrode, a platinum wire counter electrode, and a silver wire reference electrode were employed, and the ferrocene/ferrocenium (Fc/Fc^+) redox couple was used as the reference for all measurements. Atomic force microscopy (AFM) images were obtained using a Veeco NanoManVS+Multimode microscope in the tapping mode. Transmission electron microscopy (TEM) specimens were prepared following conditions identical to those of the actual devices, but they were drop-cast onto a 30 nm PEDOT:PSS-covered substrate. After drying, the substrates were transferred to deionized water and the floated films were transferred onto TEM grids. TEM images were obtained on JEOL/JEM-F200 TEM. Gel permeation chromatography (GPC) curves were performed on Agilent 1260 Infinity II chromatograph using $CHCl_3$ as an eluent at room temperature. In-situ UV-vis absorption spectroscopy measurements were performed by the FLAME-T-VIS-NIR-ES spectrometer.

2 Device fabrication

The OSC devices were fabricated with a structure of ITO/PEDOT:PSS/active layer/PDINN/Ag. The indium tin oxide (ITO) substrates (10 Ω/sq) were cleaned by sequential ultrasonic treatment in detergent, deionized water and isopropanol. Then the dried ITO substrates were treated with an ultraviolet-ozone chamber for 25 min. A thin layer of PEDOT: PSS was prepared on precleaned ITO glass through spin-coating a PEDOT: PSS aqueous solution (Heraeus-Clevios PVP Al 4083 from Xi'an Polymer Light Technology Corp., China) at 4500 r/min and baked subsequently at 150 °C for 15 min in the air. The substrates were then transferred into a N_2-filled glovebox. A blend solution was prepared by dissolving the polymer donor and acceptor in chloroform with the same optimal donor/acceptor weight ratios of 1:1.2 for blends with a total concentration of 16 mg/mL. After adding the third component with a mass proportion of 2% and the 1,8-diiodooctane (DIO) with a volume proportion of 0.25%, the blend solution was spin-coated at 3500 r/min onto the PEDOT: PSS layer. After spin-coating, the active layers were annealed at 90 °C for 10 min. Then, methanol solution of PDINN at a concentration of 1 mg/mL is spin-coated at 3000 r/min to afford a cathode buffer layer. Finally, cathode metal Ag was deposited. The photoactive layer effective area of the device was 4.8 mm^2.

3 Measurements

The current density−voltage (*J*−*V*) characteristics of the OSCs were measured under 100 mW/cm^2 air mass, AM 1.5 G spectra with a solar simulator (SS-F5, Enlitech). The light intensity was calibrated by a silicon photodiode with a KG5 filter certified by the National Renewable Energy Laboratory. The EQE spectra measurements were performed on a commercial EQE measurement system (QE-R3011, Enlitech). The light intensity at each wavelength was calibrated with a standard single-crystal Si photovoltaic cell. The charge mobilities of the devices are measured with the device structure of ITO/PEDOT: PSS/BHJ/MoO_3 (10 nm)/Ag for hole mobility and ITO/ZnO/BHJ/PDINN/Ag for electron mobility. The hole and electron mobilities are calculated according to the space-charge-limited current (SCLC) method equation $J=(9/8)\varepsilon_0\varepsilon_r\mu(V^2/d^3)$, where J is the current density, ε_0 is the dielectric constant of empty space, ε_r is the relative dielectric constant of photoactive layer materials, μ is the charge mobility, V is the internal voltage in the device, and $V=V_{appl}-V_{bi}-V_s$, where V_{appl} is the voltage applied to the devices, and V_{bi} is the built-in voltage resulting from the relative work function difference between the two electrodes, V_s is the voltage drop from the series resistance and d is the thickness of the photoactive layers.

4 Materials and synthesis

Source of raw materials: Monomer M1, BDT-2Cl-2Sn, and BDT-4F-2Sn were synthesized according to the reported literature. Tetrakis(triphenylphosphine)palladium was purchased from stream chemicals. The analytical reagent was purchased from Sinopharm Chemical Reagent Co., Ltd. Toluene is further dehydrated in the condition of sodium metal and benzophenone.

TPQ-2F-2Cl: BDT-2Cl-2Sn (131.0 mg, 0.130 mmol), M1 (120.0 mg, 0.130 mmol), and $Pd(PPh_3)_4$ (7.5 mg, 0.0065 mmol) were dissolved in 10 mL toluene and refluxed for 8 h. After cooling down to the room temperature, the mixture was poured into the 100 mL methanol and then stirred for 0.5 h. Whereafter, the precipitate was collected and extracted in the order of methanol, hexane, acetone, and chloroform. Subsequently, the polymer solution was removed chloroform solvent by rotary evaporation to obtain atropurpureus lamellar solid TPQ-0F (135.0 mg, 69 %).

TPQ-2F-4F: TPQ-2F-4F was obtained with compound BDT-4F-2Sn (142.6 mg, 0.146 mmol) following the general procedure described above. (Atropurpureus lamellar solid, 156.3 mg, 71 %).

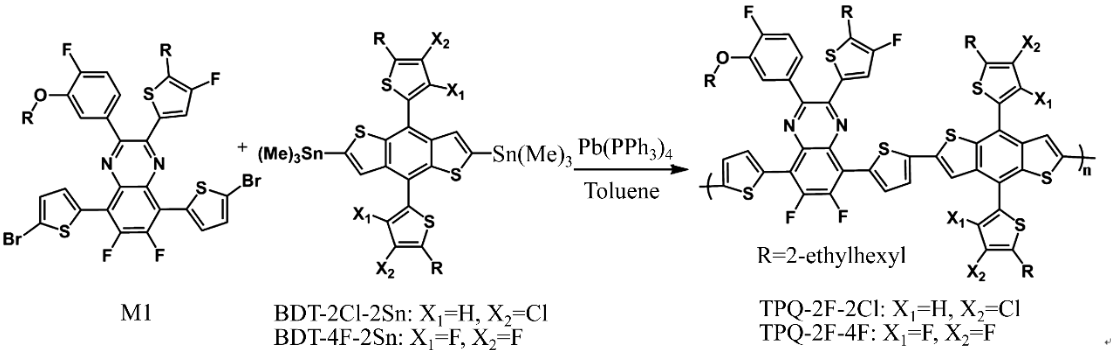

Figure S1 Synthetic routes of TPQ-2F-2Cl and TPQ-2F-4F

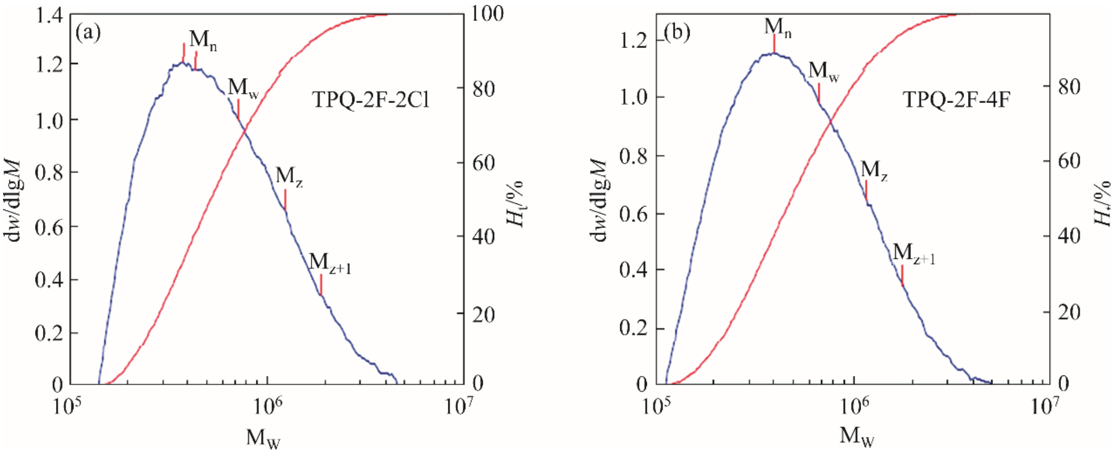

Figure S2 Gel permeation chromatography (GPC) curves of TPQ-2F-2Cl (a) and TPQ-2F-4F (b)

Table S1 GPC data summary of TPQ-2F-2Cl and TPQ-2F-4F

Material	M_n	M_w	M_v	M_z	PDI
TPQ-2F-2Cl	26008	40507	38129	54976	1.56
TPQ-2F-4F	24812	36434	34564	47595	1.47

Note: M_n is number-average molecular weight; M_w is molecular weight; M_v is viscosity average molecular weight; M_z is z-average molecular weight; PDI is polymer dispersity index.

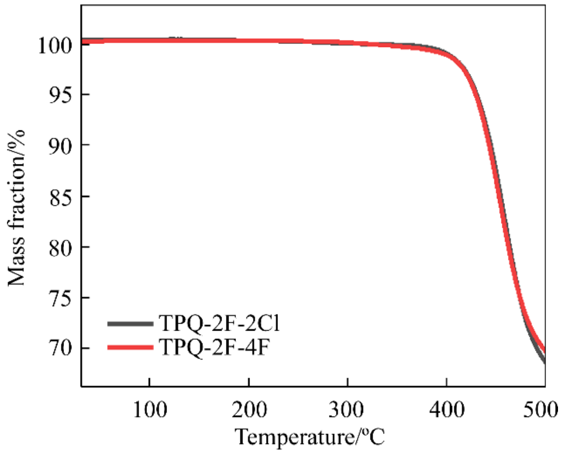

Figure S3 TGA curves of TPQ-2F-2Cl and TPQ-2F-4F

Table S2 Optical properties and energy levels of TPQ-2F-2Cl and TPQ-2F-4F

Material	$\lambda_{max}{}^{a}$/nm	$\lambda_{max}{}^{b}$/nm	$\lambda_{onset}{}^{b}$/nm	HOMO/eV	LUMO/eV	$E_g{}^{cv}$/eV	$E_g{}^{opt}$/eV
TPQ-2F-2Cl	592	601	712	−5.68	−3.49	2.19	1.74
TPQ-2F-4F	600	621	707	−5.67	−3.48	2.19	1.73

Note: [a] Absorption spectra in chloroform solution; [b] Absorption spectra in chloroform-casted films; λ_{max} is maximum absorption wavelength; λ_{onset} is absorption onset; $E_g{}^{cv}$ is electrochemical band gap; $E_g{}^{opt}$ is optical band gap.

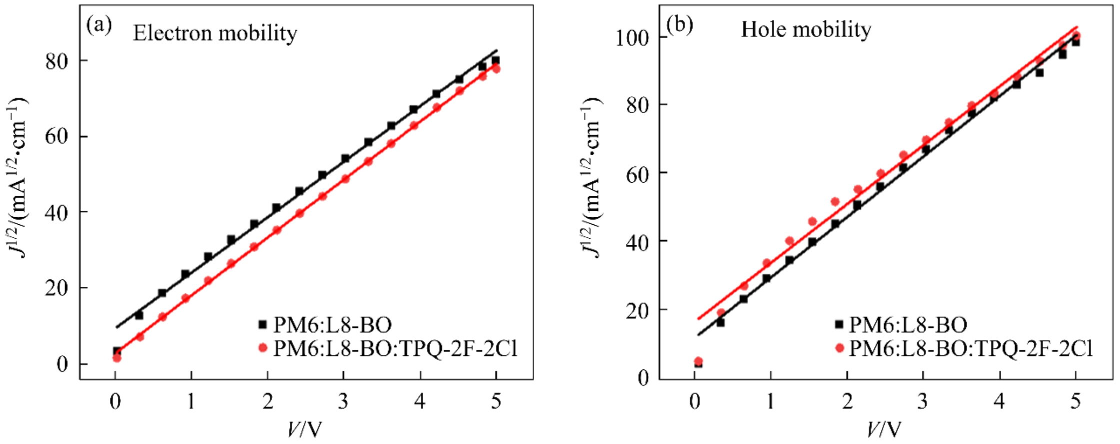

Figure S4 The electron mobility (a) and hole mobility (b) of devices based on PM6:L8-BO and PM6:L8-BO:TPQ-2F-2Cl

Table S3 Contact angle, surface tension of individual materials, and interfacial tension (γ)

Material X	Contact angle with water/(°)	Contact angle with EG/(°)	Surface tension[a]/(mN·m^{-1})	γ between X and PM6/(mN·m^{-1})	γ between X and L8-BO/(mN·m^{-1})
PM6	102.45	74.00	27.41	—	0.22
L8-BO	94.74	63.75	32.53	0.22	—
TPQ-2F-2Cl	98.24	69.50	28.66	0.01	0.12
TPQ-2F-4F	97.99	72.00	24.98	0.06	0.50

[a] Calculated using contact angles based on water and EG.

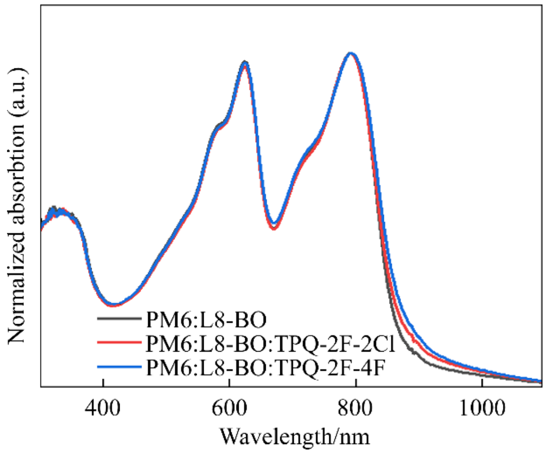

Figure S5 Normalized absorption spectra of PM6:L8-BO, PM6:L8-BO:TPQ-2F-2Cl and PM6:L8-BO:TPQ-2F-4F blend films

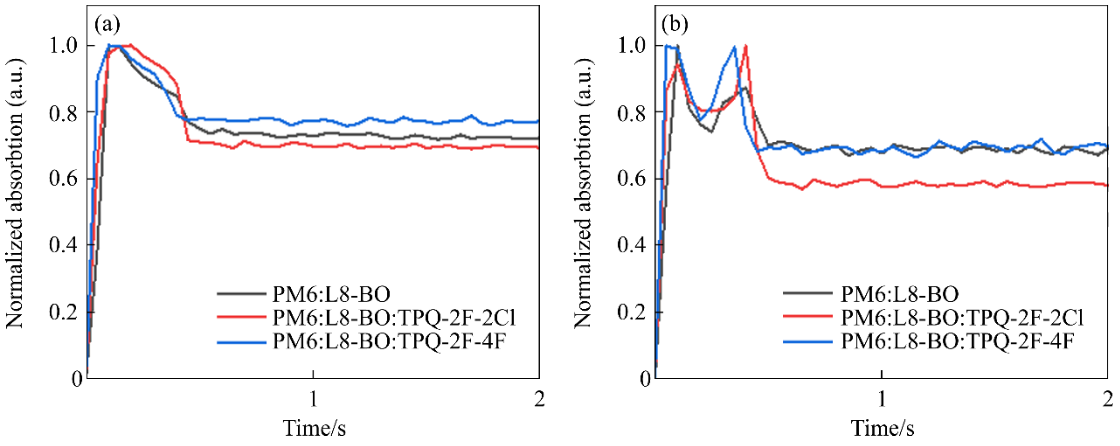

Figure S6 Normalized absorption time evolution at (a) 622 nm and (b) 790 nm for PM6:L8-BO, PM6:L8-BO: TPQ-2F-2Cl and PM6:L8-BO: TPQ-2F-4F blend films

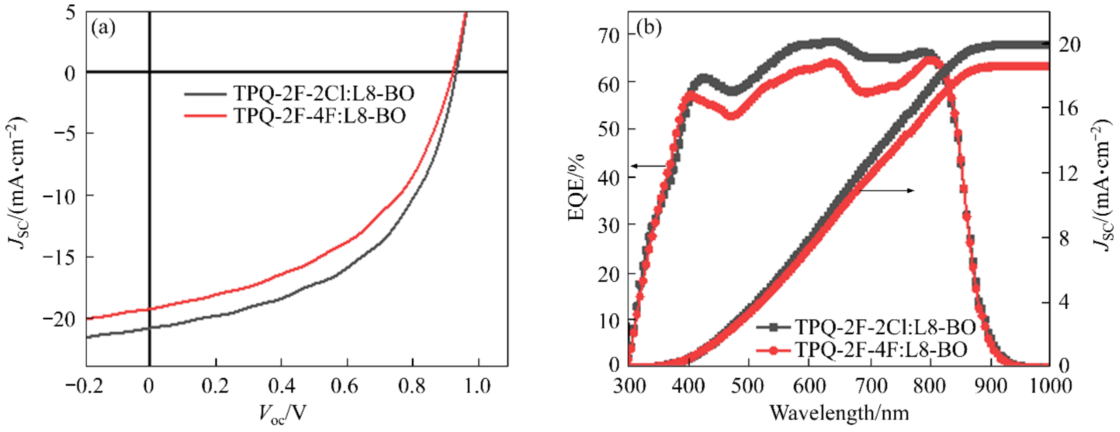

Figure S7 (a) *J*–*V* curves and (b) EQE curves of TPQ-2F-2Cl:L8-BO and TPQ-2F-4F:L8-BO blends

Table S4 Summary of binary OSCs device parameters based on TPQ-2F-2Cl:L8-BO and TPQ-2F-4F:L8-BO blends

Active layer	V_{oc}/V	J_{sc}/(mA·cm^{-2})	J_{sc}^{a}/(mA·cm^{-2})	FF/%	PCE/%
TPQ-2F-2Cl:L8-BO	0.93	20.76	19.88	50.3	9.74
TPQ-2F-4F:L8-BO	0.92	19.23	18.57	47.2	8.37

[a] Integrated current density based on EQE curves.